

NPS-SP-12-002



**NAVAL  
POSTGRADUATE  
SCHOOL**

**MONTEREY, CALIFORNIA**

**REPORT OF NAPSAT1 BATTERY THERMAL CONTACT  
RESISTANCE TESTING, MODELING AND SIMULATION**

by

Daniel Sakoda, Ronald Phelps, LT Bryce Donovan, USN

October 2012

**Approved for public release; distribution is unlimited**

THIS PAGE INTENTIONALLY LEFT BLANK

<b>REPORT DOCUMENTATION PAGE</b>				<i>Form Approved OMB No. 0704-0188</i>
<p>Public reporting burden for this collection of information is estimated to average 1 hour per response, including the time for reviewing instructions, searching existing data sources, gathering and maintaining the data needed, and completing and reviewing this collection of information. Send comments regarding this burden estimate or any other aspect of this collection of information, including suggestions for reducing this burden to Department of Defense, Washington Headquarters Services, Directorate for Information Operations and Reports (0704-0188), 1215 Jefferson Davis Highway, Suite 1204, Arlington, VA 22202-4302. Respondents should be aware that notwithstanding any other provision of law, no person shall be subject to any penalty for failing to comply with a collection of information if it does not display a currently valid OMB control number.</p> <p><b>PLEASE DO NOT RETURN YOUR FORM TO THE ABOVE ADDRESS.</b></p>				
<b>1. REPORT DATE (DD-MM-YYYY)</b> 16-10-2012	<b>2. REPORT TYPE</b> Technical Report			<b>3. DATES COVERED (From-To)</b> 19-01-2012 to 16-10-2012
<b>4. TITLE AND SUBTITLE</b>  Report of NPSAT1 Battery Thermal Contact Resistance Testing, Modeling and Simulation			<b>5a. CONTRACT NUMBER</b>	
			<b>5b. GRANT NUMBER</b>	
			<b>5c. PROGRAM ELEMENT NUMBER</b>	
<b>6. AUTHOR(S)</b>  Daniel Sakoda, Ronald Phelps and LT Bryce Donovan, USN			<b>5d. PROJECT NUMBER</b>	
			<b>5e. TASK NUMBER</b>	
			<b>5f. WORK UNIT NUMBER</b>	
<b>7. PERFORMING ORGANIZATION NAME(S) AND ADDRESS(ES) AND ADDRESS(ES)</b> Naval Postgraduate School, Space Systems Academic Group Code (SP) Monterey, CA 93943			<b>8. PERFORMING ORGANIZATION REPORT NUMBER</b> NPS-SP-12-002	
<b>9. SPONSORING / MONITORING AGENCY NAME(S) AND ADDRESS(ES)</b>  Naval Postgraduate School, Space Systems Academic Group Code (SP) Monterey, CA 93943			<b>10. SPONSOR/MONITOR'S ACRONYM(S)</b> SSAG	
			<b>11. SPONSOR/MONITOR'S REPORT NUMBER(S)</b>	
<b>12. DISTRIBUTION / AVAILABILITY STATEMENT</b> Approved for public release; distribution unlimited				
<b>13. SUPPLEMENTARY NOTES</b>				
<b>14. ABSTRACT</b> <p>Thermal modeling is an important part of spacecraft design, especially where critical components have narrow operating temperature limits. For the Naval Postgraduate School's NPSAT1 spacecraft, the lithium ion battery is the spacecraft component with the smallest temperature range of 0°C to 45°C during operation. Thermal analysis results, however, can only provide adequate results if there is sufficient fidelity in thermal modeling. Arguably, the values used in defining thermal coupling for components are the most difficult to estimate because of the many variables that define them. This document describes the work performed by the authors starting in the 2012 winter quarter as part of the SS3900 directed study course. The objectives of the study were to determine an adequate thermal model of the NPSAT1 battery as a lumped capacitance model, and an appropriate value of thermal resistance between the battery and its mounting surface for three thermal interfaces: metal-to-metal (bolted interface), Kapton®, and Choetherm® 1671. These objectives were performed through testing in a thermal-vacuum chamber with controlled boundary conditions. Modeling and simulation using the NX I-DEAS Thermal Model Generator software was performed to duplicate the test results in simulation. Agreement between the simulations and testing was achieved with differences ranging between +4°C and -8°C for the metal-to-metal interface, to as low as +2°C to -1°C using an elastomeric thermal interface material (Choetherm® 1671). The test-validated thermal model can then be incorporated into the larger NPSAT1 thermal model to specifically evaluate battery temperatures for various flight operations.</p>				
<b>15. SUBJECT TERMS</b> NPSAT1, Small Satellite, Thermal-Vacuum Testing, Thermal Modeling, Lumped Capacitance, Lithium-ion Battery				
<b>16. SECURITY CLASSIFICATION OF:</b>		<b>17. LIMITATION OF ABSTRACT</b>	<b>18. NUMBER OF PAGES</b>	<b>19a. NAME OF RESPONSIBLE PERSON</b> Daniel Sakoda
a. REPORT Unclassified	b. ABSTRACT Unclassified	c. THIS PAGE Unclassified	UU 37	<b>19b. TELEPHONE NUMBER (include area code)</b> 831-656-3198

Standard Form 298 (Rev. 8-98)  
Prescribed by ANSI Std. Z39.18

THIS PAGE INTENTIONALLY LEFT BLANK

**NAVAL POSTGRADUATE SCHOOL  
Monterey, California 93943-5000**

Daniel T. Oliver  
President

Leonard A. Ferrari  
Executive Vice President and  
Provost

The report entitled “*Report of NPSAT1 Battery Thermal Contact Resistance Testing, Modeling and Simulation*” was prepared for the Naval Postgraduate School Space Systems Academic Group.

**Further distribution of all or part of this report is authorized.**

**This report was prepared by:**

Daniel Sakoda  
Research Associate

Ronald Phelps  
Electrical Engineer

Bryce Donovan  
LT, USN

**Reviewed by:**

Rudolf Panholzer  
Chairman,  
Space Systems Academic Group

**Released by:**

Jeffrey D. Paduan  
Vice President and  
Dean of Research

THIS PAGE INTENTIONALLY LEFT BLANK

## TABLE OF CONTENTS

I.	Background .....	1
A.	INTRODUCTION.....	1
B.	PURPOSE AND OBJECTIVES .....	1
C.	LITHIUM-ION BATTERY DESCRIPTION .....	2
1.	Lithium Ion Battery Cell Specifications.....	3
2.	Battery Heaters.....	4
D.	THERMAL DISCUSSION .....	4
1.	Thermal Contact Conductance .....	6
2.	Gray Body Radiation in an Enclosure.....	7
3.	Biot Number.....	8
II.	Test Method .....	10
A.	TEST SETUP.....	10
B.	BATTERY THERMAL CAPACITANCE TEST .....	12
C.	EXPERIMENTAL THERMAL BOUNDARY CONDITIONS .....	14
D.	THERMAL INTERFACES .....	14
1.	Metal-to-Metal .....	15
2.	Kapton® Film .....	15
3.	CHOTHERM® Material .....	16
III.	Thermal Modeling and Results.....	16
A.	THERMAL MODELING .....	16
1.	Thermal Capacitance Test and Simulation .....	17
2.	Metal-to-Metal Interface Test and Simulation.....	18
3.	Kapton® Interface Test and Simulation.....	20
4.	Chotherm® Interface Test and Simulation .....	21
B.	COMPARISON OF RESULTS AND SUMMARY .....	23
IV.	Conclusions .....	23
V.	References .....	24
	INITIAL DISTRIBUTION LIST .....	25

THIS PAGE INTENTIONALLY LEFT BLANK

## LIST OF FIGURES

Figure 1. Lithium-Ion Battery Assembly.....	3
Figure 2. Battery Heater Element and Wiring Diagram.....	4
Figure 3. NPSAT1 Spacecraft Configuration (Expanded View).....	5
Figure 4. Battery Bottom View (Mounting Surface). ....	7
Figure 5. Battery Internal Temperatures for Cold Boundary Condition (Metal-to-Metal)....	9
Figure 6. Battery Thermocouple Layout (cells shown hatched).....	10
Figure 7. Internal Battery Assembly.....	11
Figure 8. Battery Test Setup.....	12
Figure 9. Battery in TVAC Chamber for Thermal Capacitance Test.....	13
Figure 10. Battery Thermal Capacitance Data ( $C_t$ ). ....	13
Figure 11. Overview of Experiment Setup and Thermal Modeling. ....	14
Figure 12. Kapton® Film on Boundary Condition Plate. ....	15
Figure 13. CHOTHERM® Interface Material on Boundary Condition Plate.....	16
Figure 14. Simulation and Test Results for Battery Thermal Capacitance. ....	17
Figure 15. Battery Thermal Model. ....	18
Figure 16. Simulation and Test Results for Metal-to-Metal Interface (LN2 Cooling). ....	19
Figure 17. Simulation and Test Results for Metal-to-Metal Interface (Heating). ....	19
Figure 18. Simulation and Test Results for Kapton® Interface (LN2 Cooling). ....	20
Figure 19. Simulation and Test Results for Kapton® Interface (Heating). ....	21
Figure 20. Simulation and Test Results for Chotherm® Interface (LN2 Cooling).....	22
Figure 21. Simulation and Test Results for Chotherm® Interface (Heating).....	22

## LIST OF TABLES

Table 1. Battery Bolted Joint Contact Conductance. ....	7
Table 2. Summary of Thermal Interface Resistances.....	23

THIS PAGE INTENTIONALLY LEFT BLANK

## ABSTRACT

Thermal modeling is an important part of spacecraft design, especially where critical components have narrow operating temperature limits. For the Naval Postgraduate School's NPSAT1 spacecraft, the lithium ion battery is the spacecraft component with the smallest temperature range of 0°C to 45°C during operation. Thermal analysis results, however, can only provide adequate results if there is sufficient fidelity in thermal modeling. Arguably, the values used in defining thermal coupling for components are the most difficult to estimate because of the many variables that define them. This document describes the work performed by the authors starting in the 2012 winter quarter as part of the SS3900 directed study course. The objectives of the study were to determine an adequate thermal model of the NPSAT1 battery as a lumped capacitance model, and an appropriate value of thermal resistance between the battery and its mounting surface for three thermal interfaces: metal-to-metal (bolted interface), Kapton®, and Chotherm® 1671. These objectives were performed through testing in a thermal-vacuum chamber with controlled boundary conditions. Modeling and simulation using the NX I-DEAS Thermal Model Generator software was performed to duplicate the test results in simulation. Agreement between the simulations and testing was achieved with differences ranging between +4°C and -8°C for the metal-to-metal interface, to as low as +2°C to -1°C using an elastomeric thermal interface material (Chotherm® 1671). The test-validated thermal model can then be incorporated into the larger NPSAT1 thermal model to specifically evaluate battery temperatures for various flight operations.

THIS PAGE INTENTIONALLY LEFT BLANK

## I. BACKGROUND

### A. INTRODUCTION

NPSAT1 is a low-cost, small satellite in development at the Naval Postgraduate School. The spacecraft hosts a number of experiments in spacecraft technology and space weather, and supports officer student education through space flight hardware development. The spacecraft battery is an experiment onboard NPSAT1 to test a lithium-ion battery built with commercial, off-the-shelf (COTS) cells for use in space.

Batteries are typically temperature critical components for spacecraft. In the case of NPSAT1, the battery has the strictest temperature limits of all subsystem components. For that reason, it is important to obtain accurate estimates of battery temperatures over the mission life prior to its actual launch into space. This is done by computer simulation where a thermal model of the spacecraft is developed. Boundary conditions for the spacecraft thermal model are defined by the space environment (sunlight and eclipse portions of the orbit, earth albedo, etc.) and duty cycling of the electronics for internal heat generation. A network of thermal couplings (radiation and conduction) is also needed for all components or subsystems. Determining the actual values of the thermal interfaces, however, is arguably the most challenging task, as the values depend on many variables such as the material properties of the two mating surfaces, surface roughness, preload of bolts, bolt size and material. Thermal interface materials can be used to help narrow the uncertainty of the thermal coupling value. The thermal resistance can be increased by use of a thermally isolating material or reduced with such things as thermal grease or thermally conductive materials.

### B. PURPOSE AND OBJECTIVES

This document describes work performed to estimate an appropriate value of thermal contact resistance at the battery-to-spacecraft interface for use in thermal modeling. Three different interfaces were tested in a vacuum chamber with instrumentation and control of the boundary conditions (heat input to the battery and temperature of the mounting interface). Testing in a vacuum limits the heat transport mechanism to conduction between the battery and the mounting interface, and radiation between the chamber and the battery housing. The decision of using three different interface materials was made to allow for later selection of the mounting interface depending on the mission orbital parameters and thermal analysis. As a secondary, or auxiliary payload, NPSAT1 is a payload of opportunity whose mission orbit is defined largely by the primary spacecraft.

One goal of the study is to simplify the modeling of the battery using the lumped capacitance method for the battery assembly. Although the battery is composed of various components, a lumped capacitance model could be used to estimate the *average battery temperature*, assuming there is little temperature gradient within the battery. Test results showed that this is the case, as will be discussed. The lumped capacitance method simplifies the dynamic response of the battery analogous to that of an electrical resistor-capacitor (RC) circuit with temperature difference,  $\Delta T$ , analogous to the electromotive force of voltage. In actuality, a high-fidelity thermal model of the battery would be comprised of a complex network of thermal resistances and capacitances given the various materials and interfaces that make up the battery assembly. Precise modeling is further complicated by

the fact that the lithium-ion cells have directional-dependencies for thermal conductivity. Maleki, et al. [1], show a US18650 lithium-ion cell to have thermal conductivity of about 3.4 W/m°K in the cross-plane direction, and 28 W/m°K for the in-plane direction, or longitudinal direction.

### C. LITHIUM-ION BATTERY DESCRIPTION

Figure 1 shows the NPSAT1 lithium-ion battery assembly. As can be seen, the battery is a complex assembly composed of various materials. The battery consists of 49 Sony US18650S cells connected with seven cells per series string by seven strings in parallel (7S-7P). The cells connected in series add cell voltages to support the spacecraft bus voltage requirements. The parallel strings increase the battery capacity (ampere-hours). The cells are sandwiched together to keep them in place by means of polycarbonate sheets and stainless steel fasteners. A thermally conductive elastomeric material, Chotherm®, is used between the housing and the polycarbonate sheets to help distribute heat among the battery cells. The Chotherm® comes in direct contact with the leads of the battery cells. A 5-Watt heater is installed to maintain the battery within operating temperatures should the battery get cold. Heat transfer on the hot extreme of operation is maintained by passive means as the initial thermal analysis showed the interior of the spacecraft to be below about 16°C, and even the exterior sides to be below 30°C [2].

The housing is a sealed container, nominally kept at 1 atmosphere with dry nitrogen. Although an atmosphere exists inside the battery, convection does not occur due to microgravity. Conduction will occur through the nitrogen, although its thermal conductivity is a fraction of that of the aluminum housing. A filter and pressure relief valve is installed in the event of a cell failure where venting of gas occurs. The mounting surface of the battery is on the left-hand side of the figure (not visible). The battery is fastened to the spacecraft equipment deck by six #8-32 screws to a torque value of 18 inch-pounds [2.0 N-m].

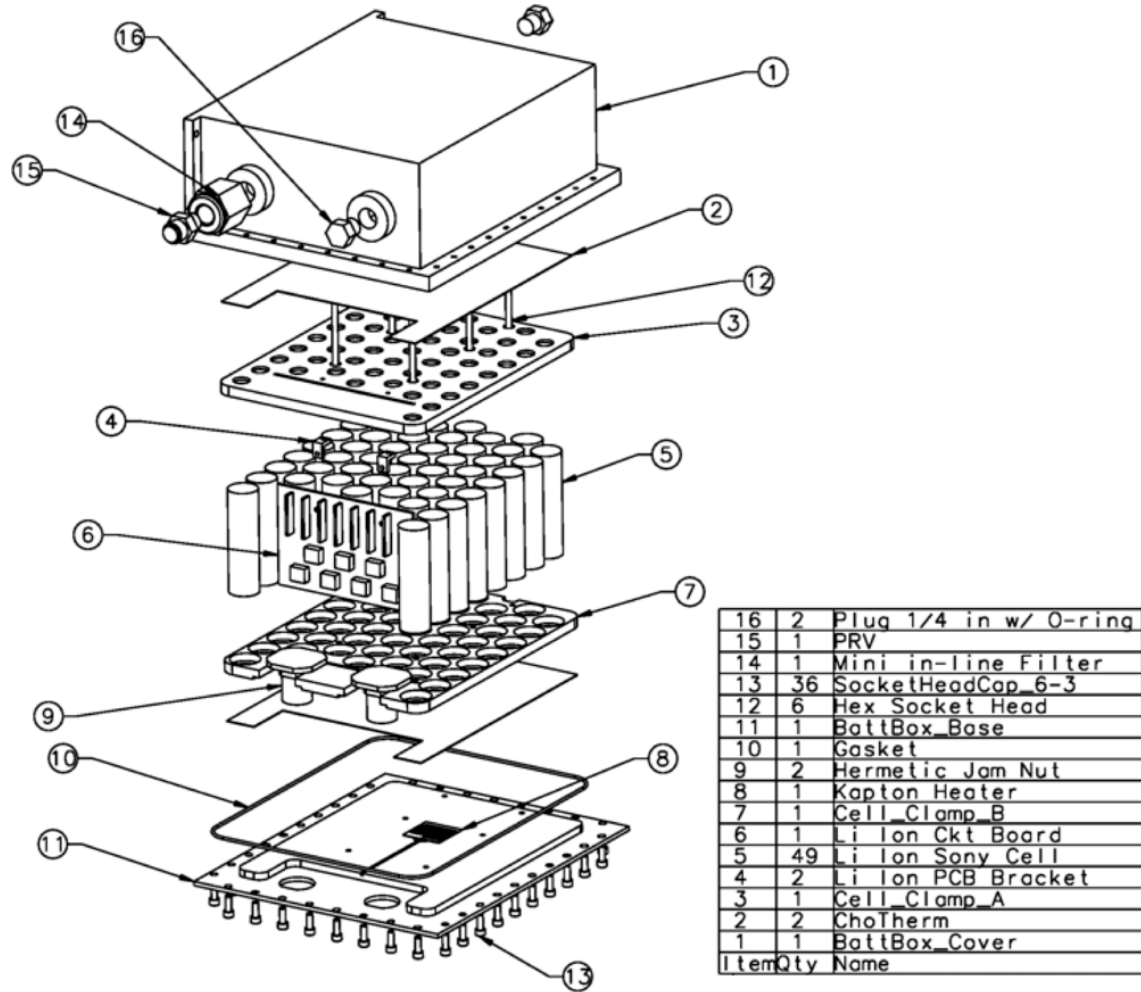


Figure 1. Lithium-Ion Battery Assembly.

## 1. Lithium Ion Battery Cell Specifications

Manufacturer temperature limits for the lithium ion battery cells are given as follows [3].

- Charge: 0°C to +45°C
- Discharge: -20°C to +60°C
- Storage: -20°C to +45°C

Representative cell specifications are given as follows.

- Charge Current: 1C/hr max. ( $C$  = cell capacity in Amp-hours)
- Discharge Current: 2C/hr max.
- Charge Voltage: 4.2±0.05 V
- Discharge Voltage: 2.5 V cutoff
- Dimensions: 18.4 mm (diameter) x 65.1 mm (height)
- Weight: 41 grams

## 2. Battery Heaters

Four heaters are located on one face of the housing. The heaters are Omegalux etched foil, heating circuits on polyimide (Kapton®) film with an adhesive side, (part number is KHLV-101/5-P). Two heaters are connected in series with two series strings connected in parallel to ensure the heaters do not exceed their specified 28 V operating voltage limit. Figure 2 shows the heater element and depicts the wiring.

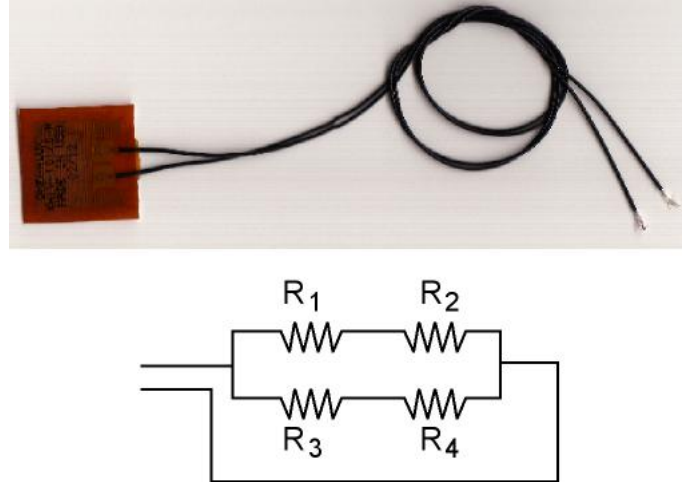


Figure 2. Battery Heater Element and Wiring Diagram.

The heaters are switched on and off by the spacecraft computer. Two thermistors are located inside the battery as control sensors. Although the mission orbit is not defined, it is expected that the spacecraft will undergo sunlight and eclipse periods. The heaters may be needed for the eclipse portion. Gruhlke presented initial heater operations for the cold case [2] of a representative circular, low-earth orbit with a beta angle of 0°, (beta angle is the angle between the sun vector and the orbital plane). Lithium-ion cells are endothermic while charging, but do generate some heat when discharging, depending on the rate of discharge as discussed by Sato [4]

## D. THERMAL DISCUSSION

Spacecraft thermal boundary conditions acting on a spacecraft include the radiation coupling with the space environment and the internal heat dissipation of the on-board electronics. The specific orbital parameters for the NPSAT1 spacecraft are as yet unknown. Nominally, the spacecraft will be placed in a circular, low earth orbit between 550 km and 650 km altitude. While in orbit, the spacecraft will be in view of the sun, the earth, and deep space. Albedo, reflected sunlight from the earth to the spacecraft, is also a heating input to the spacecraft. The orbital heating (or cooling) is a function of the radiation view factors between the spacecraft surfaces and earth, sun, and deep space depending on orientation, location, and time of year.

The predominant heat transfer mechanism for the battery is the conduction path to the equipment deck to which it is mounted. Figure 3 shows an expanded view of the NPSAT1 spacecraft with the battery located on the bottom of the third deck. Radiation also occurs

between the battery and the spacecraft internal structure and components, but, arguably, this coupling plays a minor role, as shown below. As a simplification in the overall spacecraft thermal model, internal radiation can be ignored, thereby allowing modeling of the internal components as non-geometric lumped capacitance elements. This may not hold, however, if larger temperature gradients are shown in the thermal analysis. Previous work by Gruhlke [2] shows that the temperature gradient over the mid-section of NPSAT1 is roughly within 10°C, worst-case, and this is due to half of the spacecraft in view of the sun and the opposite facing sides viewing mostly deep space. Within the volume where the battery is located, the other components and structure are within a closer temperature range. Because of the vacuum of space, as well as the gravity term in its formulation, convection is neglected. Furthermore, the battery (and other components) is treated as single isothermal masses. This assumption is reasonable if the Biot number is less than 0.1, discussed below.

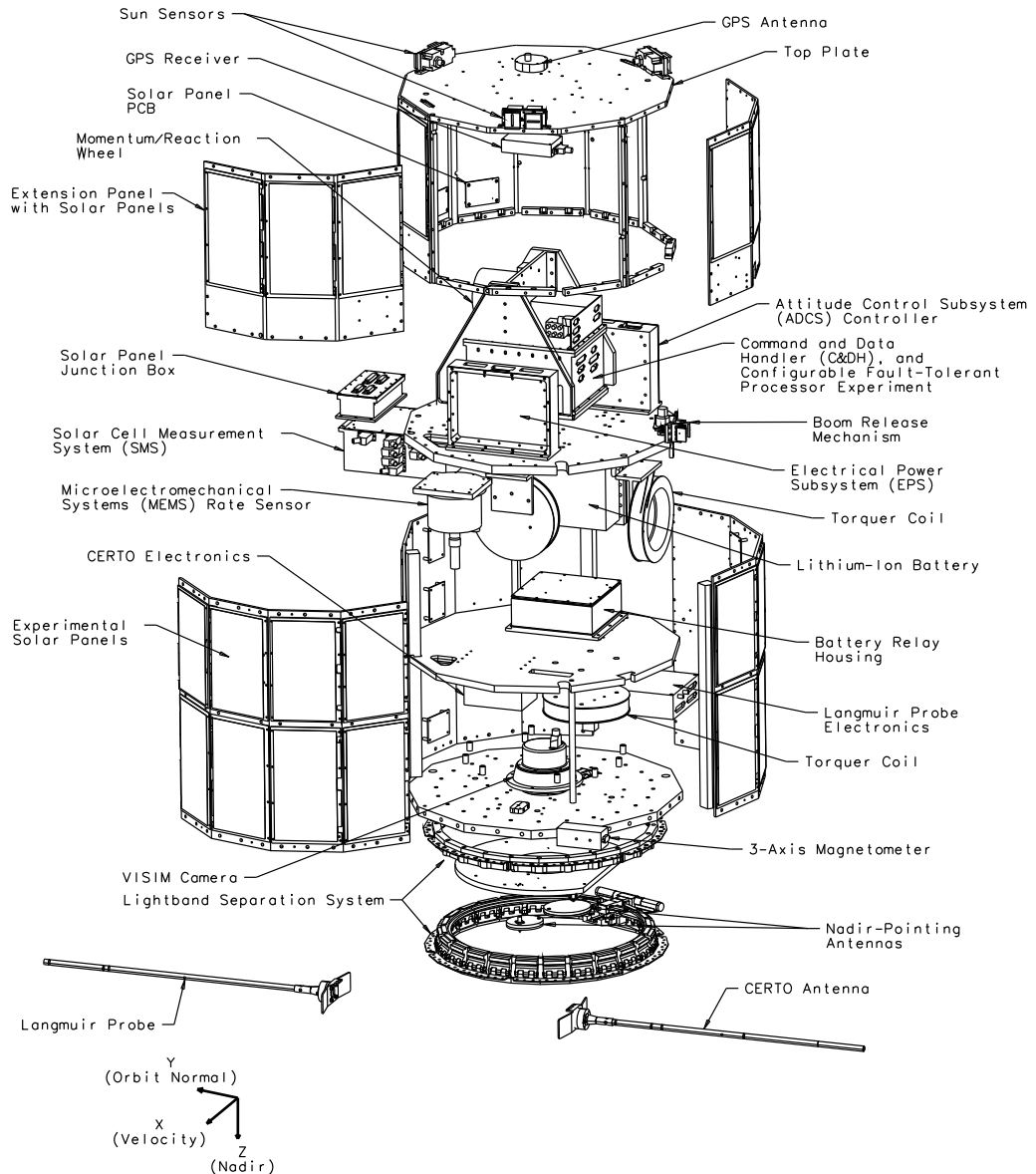


Figure 3. NPSAT1 Spacecraft Configuration (Expanded View).

## 1. Thermal Contact Conductance

The battery aluminum housing is mounted to the spacecraft equipment deck via six #8-32 stainless steel screws. Because of the metal-to-metal interface, a thermal resistance is created at the joint. A prediction of the thermal contact conductance for a bolted joint can be estimated by using the correlation provided by Gluck [5, pp. 267]<sup>\*</sup>,

$$\frac{C_b}{k_h \sigma} = 433 \left( \frac{\tau (\alpha_{al} - \alpha_{ss}) (T_p - 200)}{E \sigma^{2.5} D_s^{0.5}} \right)^{0.652}$$

where,

- $C_b$  is the bolted joint conductance [ $\text{W}/\text{°K}$ ];
- $\tau$  is the applied torque [ $\text{N m}$ ];
- $\alpha$  is the coefficient of thermal expansion (aluminum  $\alpha_{al}$ , or stainless steel  $\alpha_{ss}$ );
- $T_p$  is the plate temperature minus a lower limit of  $200^\circ\text{K}$ ;
- $E$  is the effective modulus of elasticity of the aluminum and stainless steel screw bolted joint, given by the following ( $n$  is Poisson's ratio) [ $\text{N}/\text{m}^2$ ]

$$E = \left[ \frac{(1 - \nu_{al}^2)}{E_{al}} + \frac{(1 - \nu_{ss}^2)}{E_{ss}} \right]^{-1};$$

- $\sigma$  is the combined roughness [ $\text{m}$ ];

and,

$$k_h \quad \text{is the harmonic mean of the thermal conductivities, } \left( \frac{2k_{al}k_{ss}}{k_{al} + k_{ss}} \right).$$

Using the correlation equation, and isolating for  $C_b$ , a contact conductance can be found for the bolted interface for the battery. This is given in Table 1. As is shown, the bolted-joint thermal interface is dependent on a number of parameters. Though the mounting area may be considered large, the thermal contact resistance becomes negligible outside a radius of about 1.5 times the bolt diameter ( $R_C = 1.5 D_s$ ) [5, p.268]. Figure 4 shows a bottom view of the battery assembly with the mounting interface outlined and the bolted interface thermal contact resistance area shown.

---

\* Note: corrected version has coefficient of 433 (differs from that given in [5]).

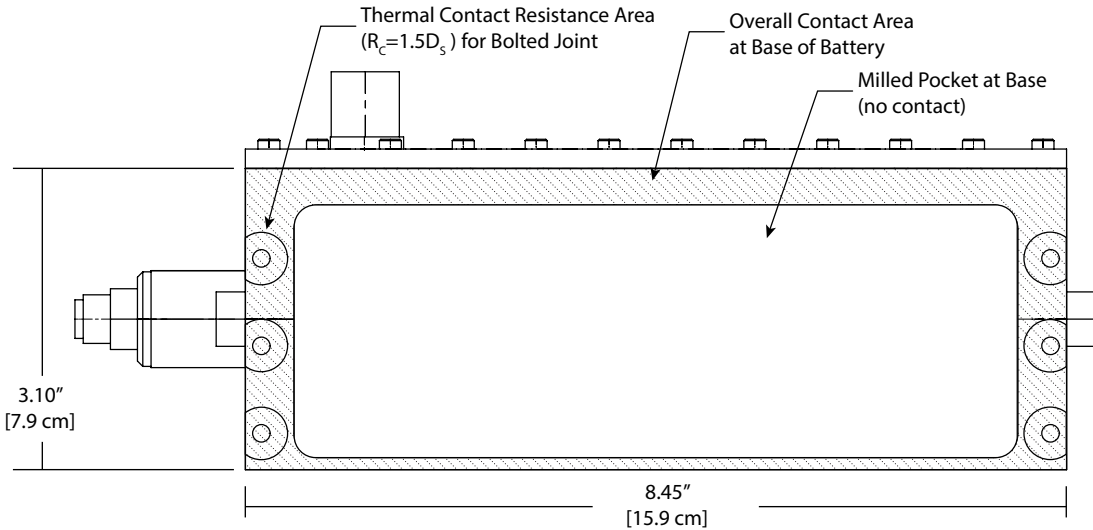


Figure 4. Battery Bottom View (Mounting Surface).

Table 1. Battery Bolted Joint Contact Conductance.

Term	Value	Units
$k_h$	29.535	W/m°K
$\sigma$	1.60E-06	m
E	5.725E+10	N/m <sup>2</sup>
$T_p$	300.	°K
$\alpha_{al}$	23.6	μm/m°K
$\alpha_{ss}$	17.3	μm/m°K
$\tau$	2.236	N-m
$C_b$	0.403	W/°K
TCR (1/C <sub>b</sub> )	2.48	°K/W

## 2. Gray Body Radiation in an Enclosure

Radiative heat transfer of the battery can be modeled as an object located inside an enclosure using the simplification of gray body radiation ( $\alpha = \varepsilon$ ). Radiative heat transfer between surfaces,  $S_i$  and  $S_j$ , is a function of the view factor between the two surfaces,  $F_{ij}$ , their temperatures,  $T_i$  and  $T_j$ , their respective areas,  $A_i$  and  $A_j$ , the respective optical properties of emissivity,  $\varepsilon$ , and the Stefan-Boltzmann's constant ( $5.670 \times 10^{-8} \text{ W/m}^2 \cdot \text{K}^4$ ).

$$q_{ij} = q_i = q_j = \frac{\sigma(T_i^4 - T_j^4)}{\frac{1-\varepsilon_i}{\varepsilon_i A_i} + \frac{1}{A_i F_{ij}} + \frac{1-\varepsilon_j}{\varepsilon_j A_j}} \quad [6, \text{ p. 738}]$$

The total exposed surface area of the battery housing is approximately 0.115 m<sup>2</sup> and the interior of the spacecraft section where the battery is mounted, excluding the other components, is 0.715 m<sup>2</sup>. Treating the battery and enclosure each as isothermal, we can simplify Eq 1 to a two-surface problem with the view factor,  $F_{ij} = 1$ . The battery aluminum housing has an iridite (chemical conversion coating) finish, and the spacecraft side panels are black anodized aluminum. The emissivity given to the battery surface is 0.11 [5]<sup>†</sup>; and that of the enclosure surface is 0.88 [5]<sup>‡</sup>. With a temperature difference of 10°C, the heat transfer is about 0.6 W. Contrasting that with the battery's bolted interface, the heat flow due to contact conduction is 13 W, using a thermal resistance of 0.75 °C/W (a value from the results of this study). This example illustrates the greater impact of conduction, and thus, the impetus to investigate the sensitivity of the battery thermal design to the bolted interface.

### 3. Biot Number

The Biot number is a test of the lumped capacitance method for the heat transfer process, and is basically the ratio of the internal thermal resistance of a solid to the thermal resistance at the boundary. In this case, the process for the battery is through radiation and conduction through the mounting interface, i.e., contact conductance. When the Biot number is much smaller than 0.1, it means the resistance to conduction within the solid material is much less than resistance to other heat transport mechanisms at the surface, and therefore the temperature gradients are small over the bulk of the material. The Biot number,  $B_i$ , is non-dimensional and given as the following for radiation:

$$B_i = \frac{h_{rad} L_C}{k}$$

where,  $h_{rad}$  is the radiation coefficient,  $L_C$  is a characteristic length given as the ratio of the solid's volume ( $l \times w \times h = 215\text{mm} \times 84 \times 159\text{mm}$ ) to surface area ( $2(w \times l) + 2(l \times h) + 2(w \times h)$ ). Here the overall dimensions are used, treating the battery as a simple box (parallel piped).  $k$  is the solid's thermal conductivity. However, as can be seen from Figure 1, the battery is composed of various materials. Choosing a low value for thermal conductivity, such as that for polycarbonate (0.19 W/m°K), will ensure a conservative estimate for the Biot number. The radiation coefficient is a function of the temperature difference between the solid,  $T_S$ , and the surrounding environment,  $T_{Surr}$ .

$$h_{rad} = \epsilon \sigma (T_S + T_{Surr}) (T_S^2 + T_{Surr}^2)$$

where,  $\epsilon$  is the emissivity of the battery surface (0.11) and  $\sigma$  is the Stefan-Boltzmann constant ( $5.67 \times 10^{-8} \text{ W/m}^2\text{K}^4$ ). Again, choosing values for the battery box temperature (-35°C) and enclosure temperature (373°C), a conservative value can be obtained for the Biot number. Substituting these conservative values for the radiation Biot number yields a value of  $3.19 \times 10^{-6}$ .

---

<sup>†</sup> This number is representative. Actual values are highly dependent on the chemical conversion coating process.

<sup>‡</sup> This number is representative. Actual values are highly dependent on the anodizing process.

The Biot number for the heat transfer process through contact conductance is given as

$$B_i = \frac{h_c t}{k_{plate}}$$

where,  $h_c$  is the contact conductance in W/m<sup>2</sup>K with its area estimated by a radius of 1.5 D<sub>S</sub> per bolt (D<sub>S</sub> = screw diameter). The mounting flange thickness is defined by 't' (0.0064 m) and k<sub>plate</sub> is the thermal conductivity of aluminum (160 W/mK). Using the bolted joint contact conductance, C<sub>b</sub>, discussed earlier, the Biot number becomes:

$$B_i = \frac{C_b t}{n\pi(1.5D_s)^2 k_{plate}}$$

where, n, is the number of screws. Substituting values yields B<sub>i</sub> = 0.022.

Testing results verified that the battery is isothermal within about ±5°C. The following figure shows the battery cell temperatures versus time. The battery is mounted to an aluminum plate with liquid nitrogen (LN2) passing through it to create a cold boundary condition for the bolted interface. The LN2 was allowed to flow for about one hour and twenty minutes. Also visible in the plot is a failed thermocouple, and another that was intermittently giving poor data. Layout of the thermocouples is shown in Figure 6

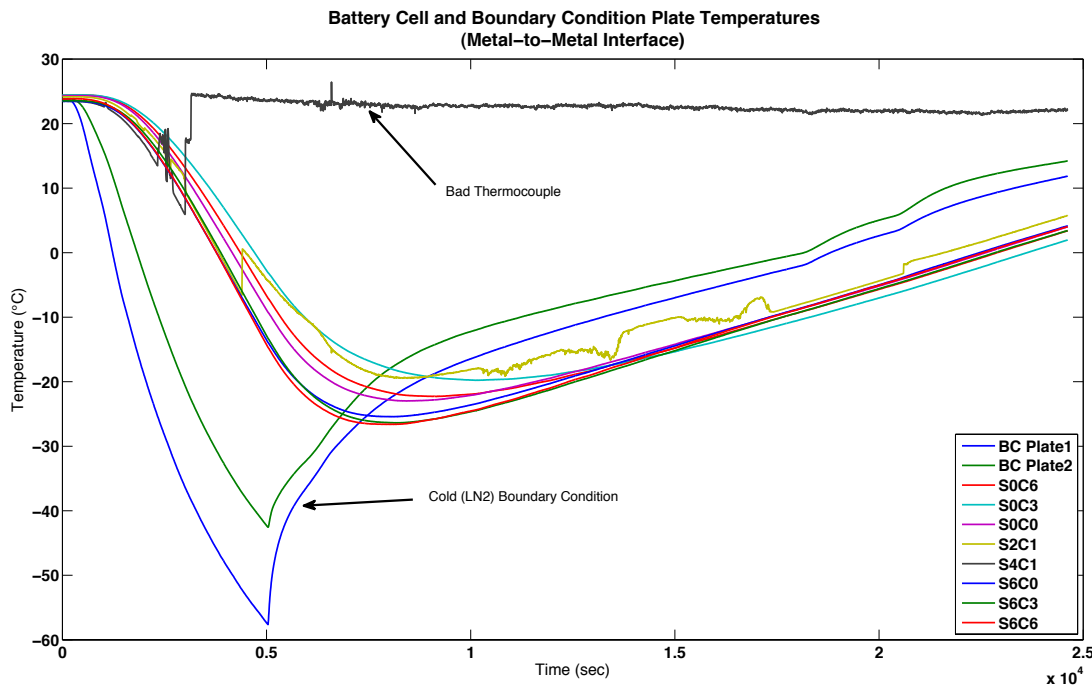


Figure 5. Battery Internal Temperatures for Cold Boundary Condition (Metal-to-Metal).

## II. TEST METHOD

### A. TEST SETUP

Testing to measure the thermal contact resistance at the mounting interface was done in a thermal-vacuum chamber to better control thermal boundary conditions. Operating in a vacuum removes any convective heat transfer, thus limiting heat transfer exclusively to radiation and conduction. The chamber was outfitted with six thermocouples to measure the temperature environment as a radiation enclosure. The battery was mounted to an aluminum plate, the “*Boundary Condition Plate*,” that was plumbed to allow the use of liquid nitrogen. Two thermocouples were attached to the plate. A dewar of liquid nitrogen was connected to valves, piping and feed-through ports allowing connection to the mounting plate, or cold plate, from outside of the chamber.

The battery assembly was modified to add eight thermocouples of a similar type as that of the thermal-vacuum chamber so that a better mapping of temperatures could be obtained for temperature gradients, and the same data acquisition system could be used. These thermocouples were attached at approximately mid-height to the perimeter of the battery pack, as depicted in Figure 6, where numbering is denoted by ‘S’ for series number and ‘C’ for cell number, i.e., S6C3 is battery cell 3 in string 6, indexing from zero. Adding thermocouples to the inner cells would have been difficult, as it would require disassembling the battery.

Thermocouple wires were fed through the housing where the filter and pressure relief valve would be mounted. The internal volume would then also be in a vacuum, however, the thermal conduction through the nitrogen gas is a small fraction of that of the solid housing and assembly. Figure 7 shows the internal battery assembly with the white Choetherm® material visible at the top. Also shown is one of the two battery thermistors (not used in the experiment).

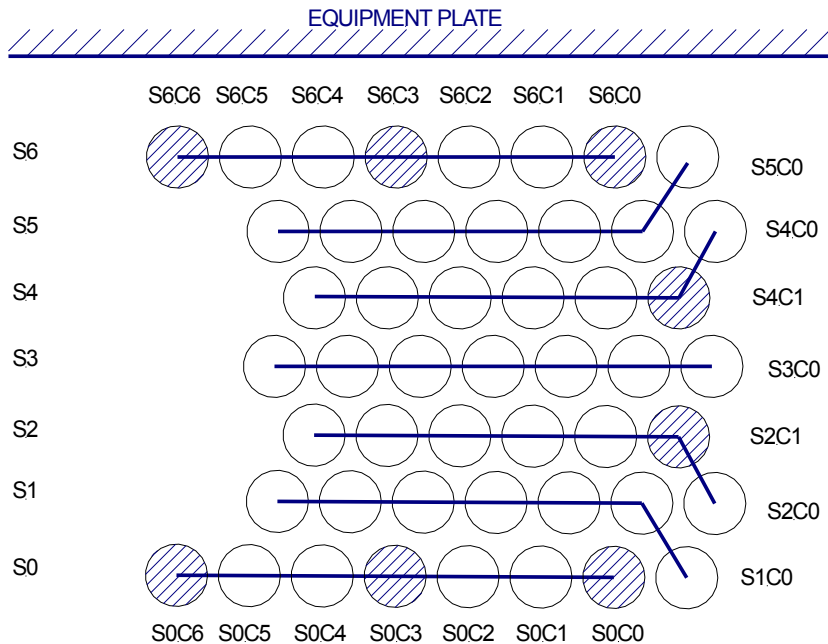


Figure 6. Battery Thermocouple Layout (cells shown hatched).

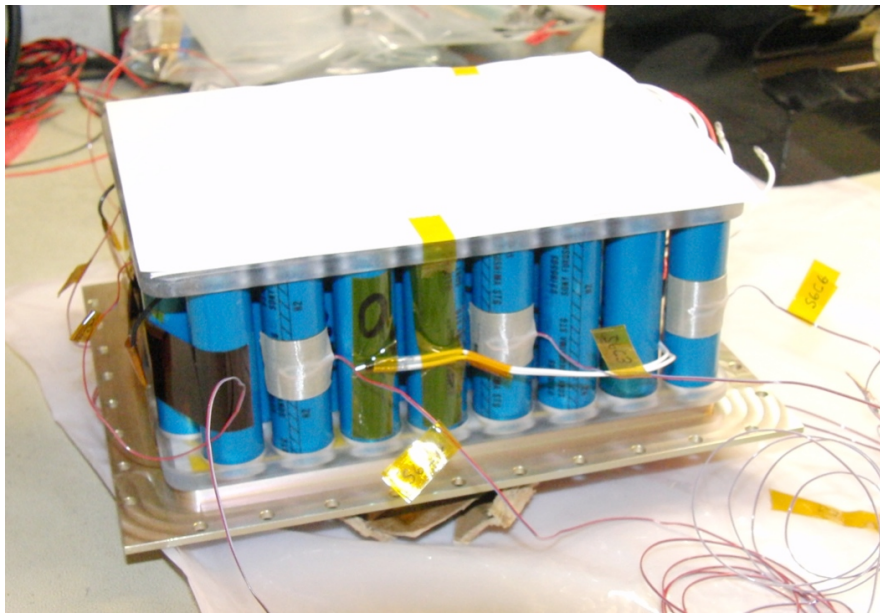


Figure 7. Internal Battery Assembly.

Figure 8 depicts how the battery mounts to the boundary condition plate. The boundary condition plate was made with the same material as that of the NPSAT1 equipment deck (aluminum 6061-T6). It has a rectangular hole in the middle of the plate to remove mass since thermal capacitance is directly related to mass. During the test, the liquid nitrogen boils off immediately and takes some time before actual liquid nitrogen is flowing through the plate. This is inconsequential, however, since the objective is to force a known transient boundary condition and measure those temperatures. The temperature profile of the boundary condition plate is then used as a time-varying temperature boundary condition in the thermal modeling.

The battery is neither charged nor discharged during the tests. As stated earlier, lithium-ion batteries are endothermic during charge and exothermic in discharge, as a function of the rate of discharge. To simplify the test and minimize the input variables for thermal modeling, the battery was left electrically inert. The only boundary conditions are that of the internal battery heaters controlled by a power supply, the boundary condition plate as a temperature boundary condition, and the thermal vacuum chamber walls as radiative coupling.

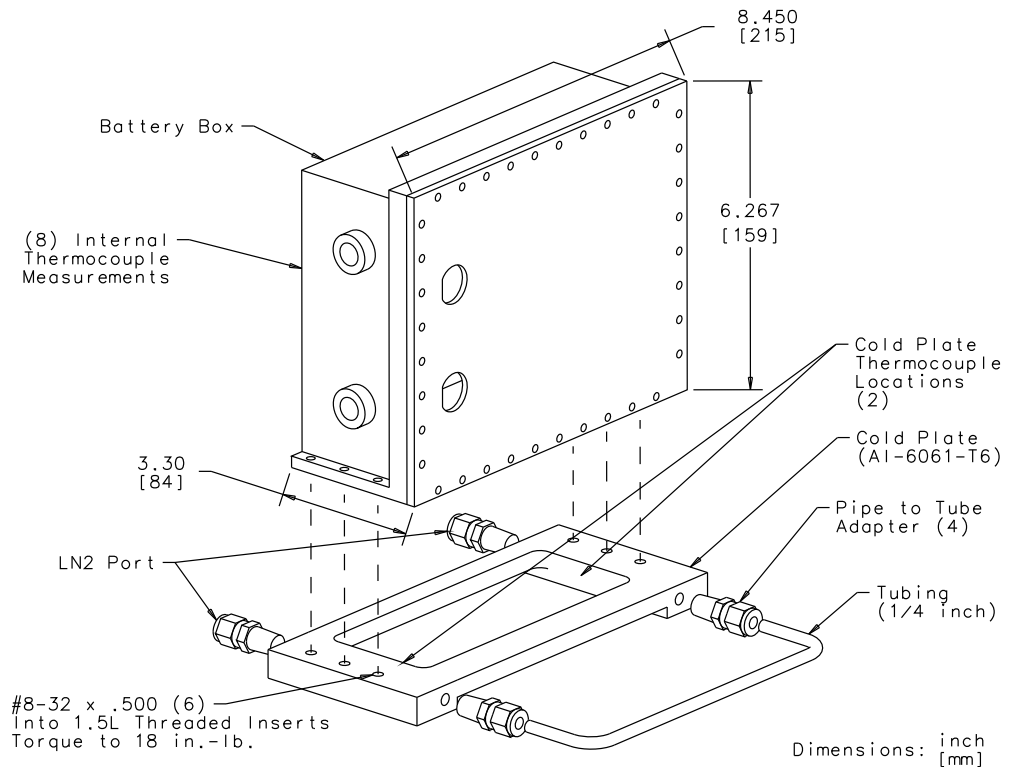


Figure 8. Battery Test Setup.

The thermal-vacuum (TVAC) chamber is outfitted with a mechanical pump for rough pumping, and a turbo-molecular pump for achieving high vacuum. The vacuum reached was less than  $10^{-5}$  Torr to as low as  $8 \times 10^{-8}$  Torr.

## B. BATTERY THERMAL CAPACITANCE TEST

A measure of the battery's thermal capacitance was done using the internal heaters and thermally isolating the battery from the chamber. The battery was placed on a polycarbonate spacer inside the TVAC chamber and allowed to reach equilibrium. At the start of data recording, all chamber and battery temperatures were within  $1^{\circ}\text{C}$ . The heaters were activated and temperatures were recorded. From the battery temperature data, the average of the six thermocouples was taken and used to determine a least-squares fit to the linear portion, the slope of which yields the heat capacity,  $C_t$ , in  $\text{J}^{\circ}\text{K}$ . The data was then used to determine the time constant,  $\tau$ , given as  $\tau = R_t C_t$ , from which  $R_t$ , the thermal resistance in  $^{\circ}\text{K}/\text{W}$ , was found.

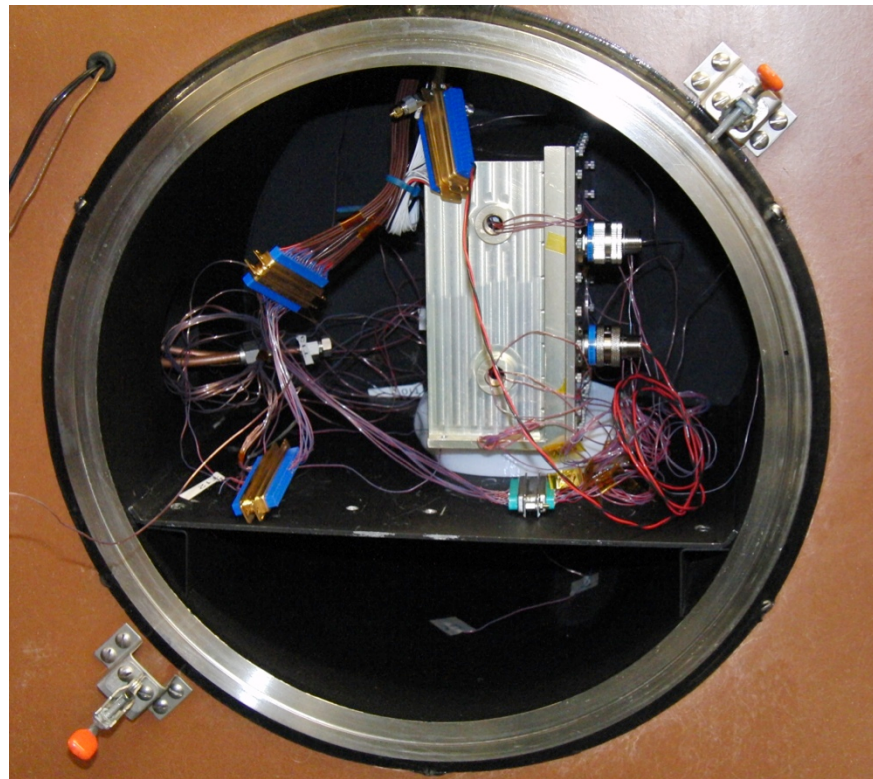


Figure 9. Battery in TVAC Chamber for Thermal Capacitance Test.

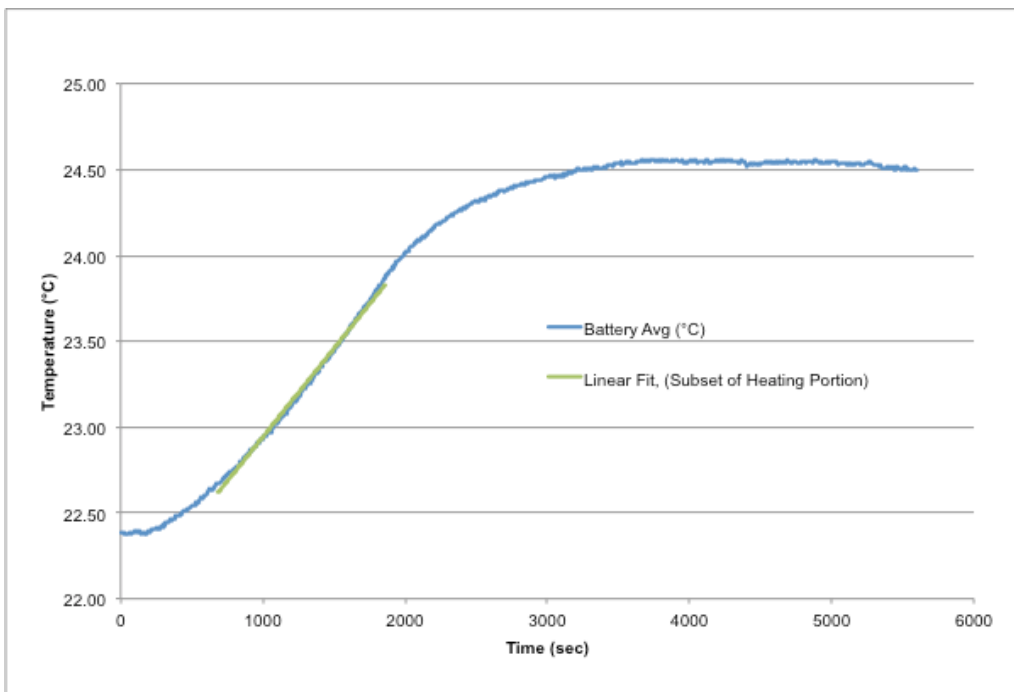


Figure 10. Battery Thermal Capacitance Data ( $C_t$ ).

### C. EXPERIMENTAL THERMAL BOUNDARY CONDITIONS

The chamber temperatures define the radiative boundary condition. The boundary condition plate temperatures and the internal heat generated define the other boundary conditions. By measuring the six temperatures of the TVAC chamber and two boundary condition plate temperatures, the average temperatures as a function of time are used as the thermal boundary condition in the thermal model simulation. Internal heat generation from the heaters was measured by recording the voltage and current inputs to the battery heaters. A stopwatch was used to determine the start and stop of the heat input.

The sample rate of the experimental data was set to 5 sec. Data was recorded and stored into a telemetry database via a data acquisition software tool developed in-house. Each temperature channel is stored with a time stamp. It is assumed that the average temperature is sufficient for this study, as the TVAC chamber and battery are isothermal.

### D. THERMAL INTERFACES

Three interfaces were tested in the TVAC chamber. The first is the bare metal-to-metal interface. The second interface tested was a .05 mm [0.002 in.] thick Kapton® film. The third interface material was a 0.38 mm [0.015 in.] thick thermally conductive elastomeric material, CHOTHERM®. In each case, the battery is mounted to the cold plate with six #8-32 (NAS1352N08) fasteners with an installation torque of 2.0 N-m [18 inch-pound].

Test data was used to estimate appropriate values for the battery thermal capacitance, resistance, and resistance of the thermal interface through use of the Siemens NX I-DEAS thermal model generator (TMG) software. Once the orbital parameters are defined, the appropriate interface material can be selected based on the spacecraft thermal analysis results. In addition, battery heater operations can be defined to maintain the battery within its operating temperature limits. Figure 11 depicts an overview of this study where experiment measurements of the boundary conditions, i.e., chamber temperature, battery heater power, and boundary condition plate temperatures, are used in the development of the computer simulation.

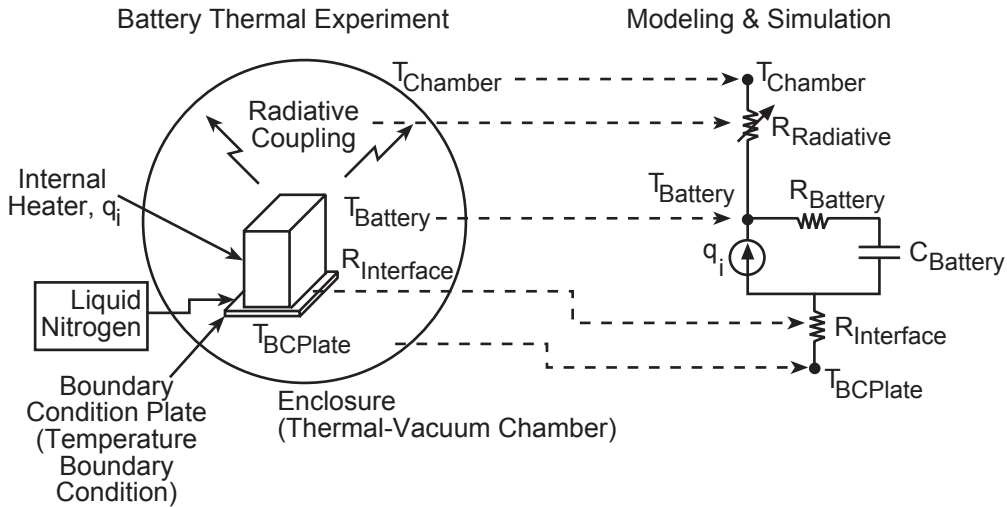


Figure 11. Overview of Experiment Setup and Thermal Modeling.

## 1. Metal-to-Metal

The metal-to-metal interface is simply the bolted interface without any thermal interface material. Therefore the thermal path is through the contact resistance due to the six bolts. The total mounting surface of the battery is only  $43.4 \text{ cm}^2$  [6.73 in<sup>2</sup>] due to a pocket located on the mounting surface. However, it should be noted the contact area further from the bolt locations contributes little due to the lack of immediate clamping force and surface roughness. As discussed, the annular region inscribed by a radius of 1.5 times the diameter of the screw ( $1.5 D_S$ ) is the predominant area for contact conductance [5, p. 263].

## 2. Kapton® Film

The use of Kapton® film between the mounting interface is intended to provide thermal insulation. Kapton® is a polyimide film with thermal conductivity of 0.12 W/m·K [7]. The 0.05 mm thick Kapton® film was cut to match the mounting interface area and to provide holes for the fasteners. Figure 12 shows the Kapton® film attached to the cold plate.

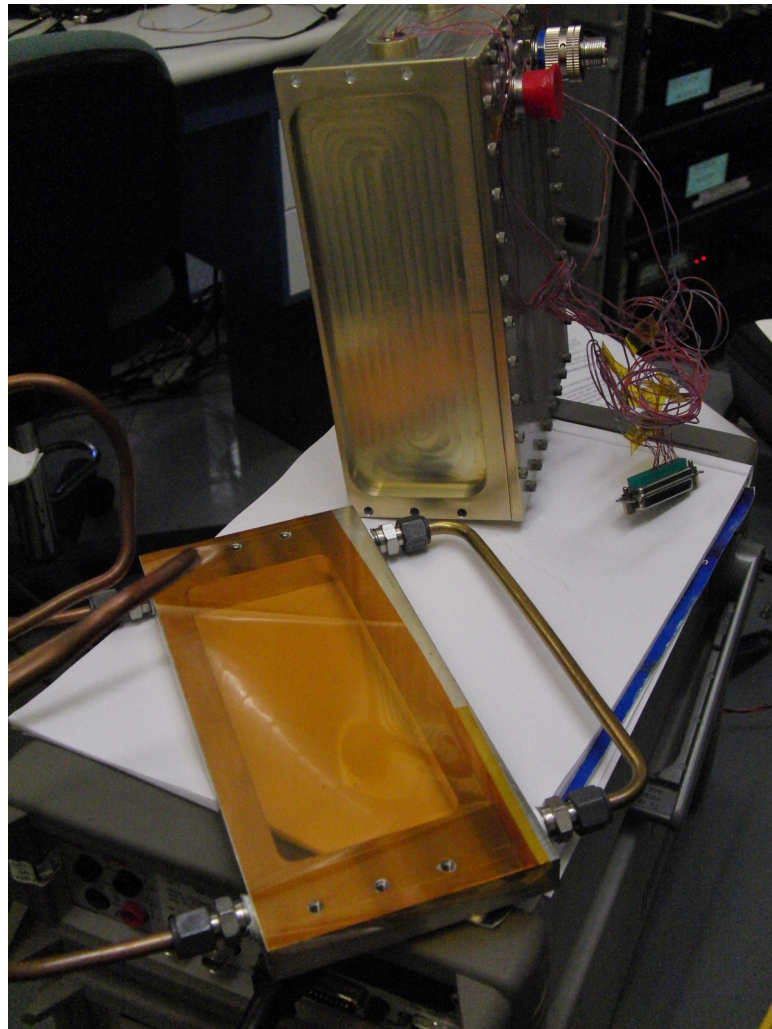


Figure 12. Kapton® Film on Boundary Condition Plate.

### 3. CHOTHERM® Material

CHOTHERM® (1671) is a thermally conductive elastomer commonly used as a thermal interface between semiconductor devices and their heat sinks. The material is a fiberglass-reinforced silicon binder with boron nitride particles dispersed within. Thermal conductivity is given as 2.6 W/m-K and thermal impedance as 1.48 °C-cm<sup>2</sup>/W [8]. Figure 13 shows the battery mounting surface and the cold plate with the CHOTHERM® material attached.

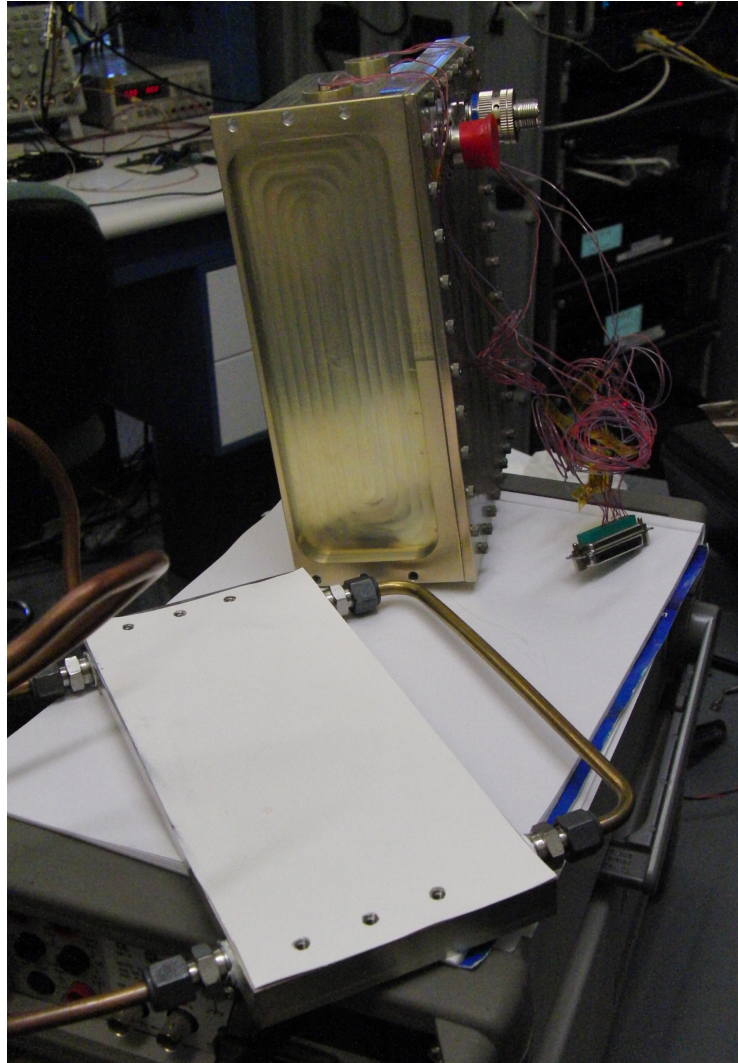


Figure 13. CHOTHERM® Interface Material on Boundary Condition Plate.

## III. THERMAL MODELING AND RESULTS

### A. THERMAL MODELING

The thermal capacitance test run was used in defining a lumped capacitance element for the battery. In modeling the battery, agreement between the simulation temperatures and the test results was used as evidence of thermal modeling validation. Given the thermal capacitance of the battery, the measured temperature boundary conditions and heating, a

thermal model of the battery-TVAC system was developed to determine the thermal resistance of the battery-to-mounting-plate (boundary condition plate) interface ( $R_{\text{Interface}}$  of Figure 11) for each of the three interface scenarios.

### 1. Thermal Capacitance Test and Simulation

The estimate of the thermal capacitance of the battery was derived from the data shown in Figure 10. A linear least squares fit estimate of the heating portion of the experiment yielded an estimated value of  $5740 \text{ J}/^{\circ}\text{C}$ . Using this value alone, however oversimplifies the model such that there is no dynamic response after the heater is turned off, i.e., no time constant. An additional element and internal resistance value were added to create a better fit between the simulation results and the experimental data. Figure 14 shows an overlay plot of the thermal capacitance run in the TVAC chamber with that of the simulation. The final lumped capacitance value for the battery is  $4550 \text{ J}/^{\circ}\text{C}$  in series with a resistor of  $1.0 \text{ }^{\circ}\text{C}/\text{W}$  and an element of  $554 \text{ J}/^{\circ}\text{C}$  thermal capacitance. This lumped capacitance model was used in the subsequent thermal modeling that included the thermal interfaces and boundary conditions recorded from the TVAC tests. Figure 15 depicts how the thermal capacitance test run was modeled using the NX I-DEAS TMG software. For the case when the battery is mounted to the boundary condition plate an additional ‘null’ element was created to work within the modeling constraints where a visible element is required to be the primary element when defining a thermal coupling. The thermal coupling between the ‘null’ element and the lumped mass element of the battery was given a very low ( $1\text{E-}14$ ) thermal resistance. This configuration is shown on the right-hand side of Figure 15.

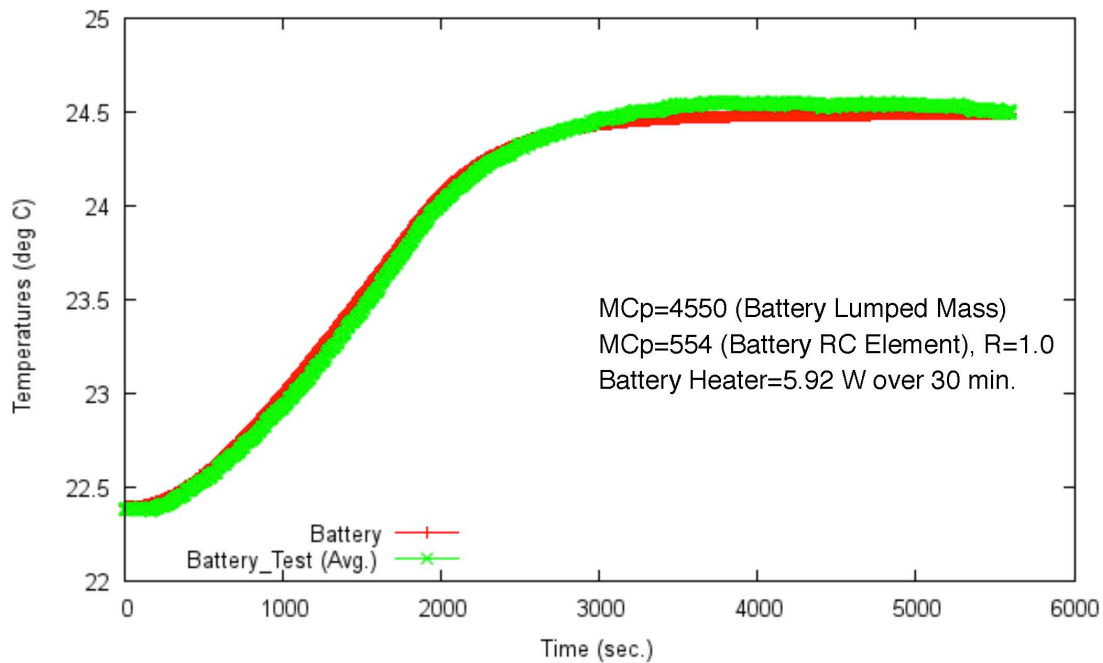


Figure 14. Simulation and Test Results for Battery Thermal Capacitance.

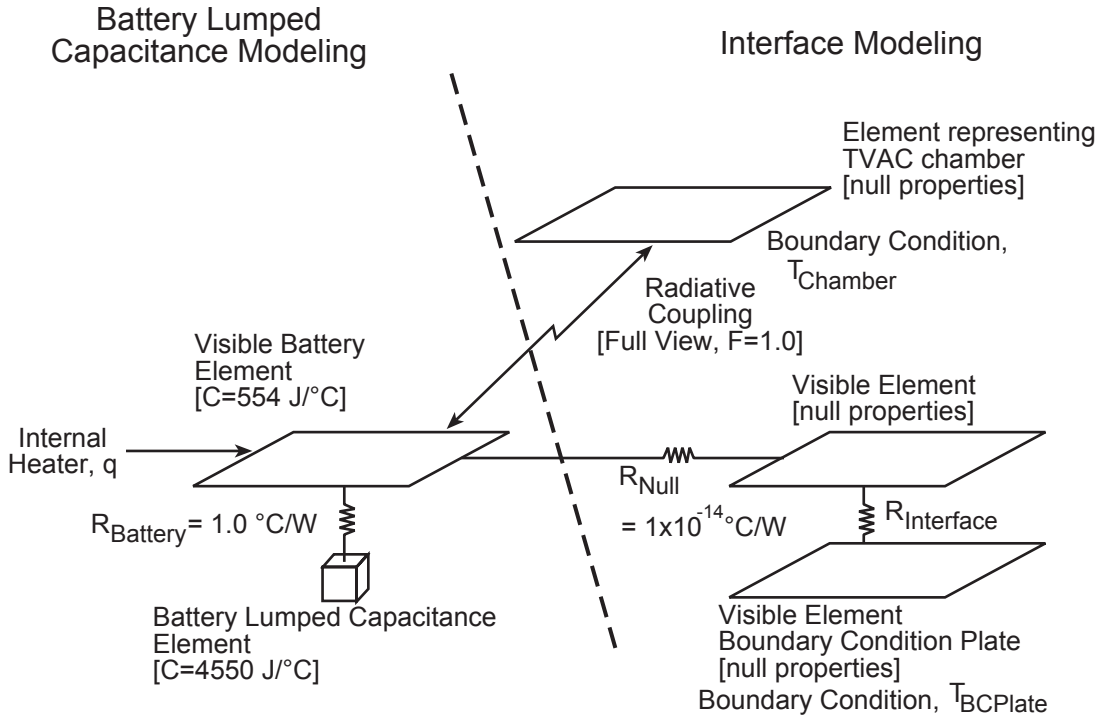


Figure 15. Battery Thermal Model.

## 2. Metal-to-Metal Interface Test and Simulation

The simulation model reflecting the metal-to-metal interface between the battery and the boundary condition plate used the identical lumped capacitance thermal model of the battery as shown in Figure 15. In this case the boundary condition plate and the thermal resistance of the interface was added. The interface thermal resistance,  $R_{\text{Metal-to-Metal}}$ , was modified, iteratively, until good agreement was achieved between the simulation results and the test results. Final estimate of the thermal resistance for this case is  $R_{\text{Metal-to-Metal}} = 0.75 \text{ }^{\circ}\text{C}/\text{W}$  as shown in Figure 16 and Figure 17.

### Battery Temperatures from Test and Simulation Metal-to-Metal Interface

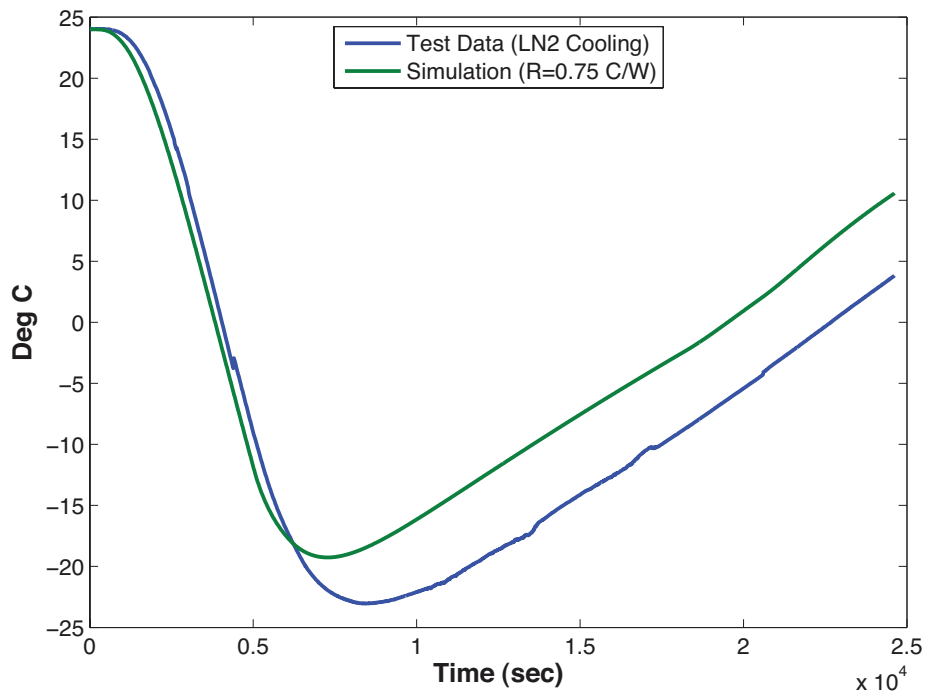


Figure 16. Simulation and Test Results for Metal-to-Metal Interface (LN2 Cooling).

### Battery Temperatures from Test and Simulation Metal-to-Metal Interface

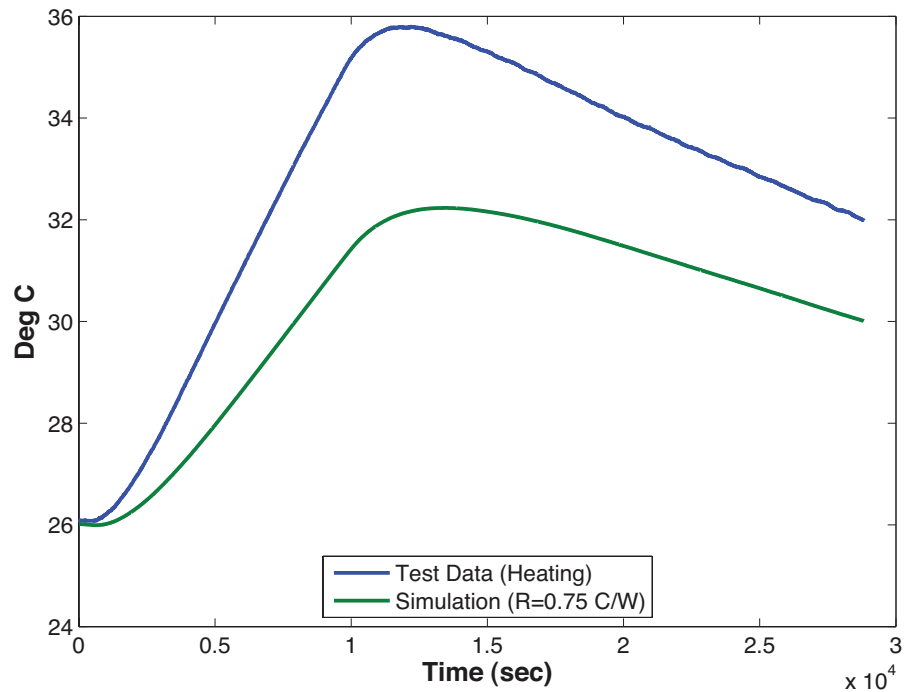


Figure 17. Simulation and Test Results for Metal-to-Metal Interface (Heating).

### 3. Kapton® Interface Test and Simulation

The thermal modeling and analysis process for the Kapton® film interface was similar to that of the metal-to-metal interface, described above. The resulting interface resistance was determined to be,  $R_{\text{Kapton}} = 1.903 \text{ }^{\circ}\text{C/W}$ . Comparison plots of the test and simulation results are shown in Figure 18 and Figure 19.

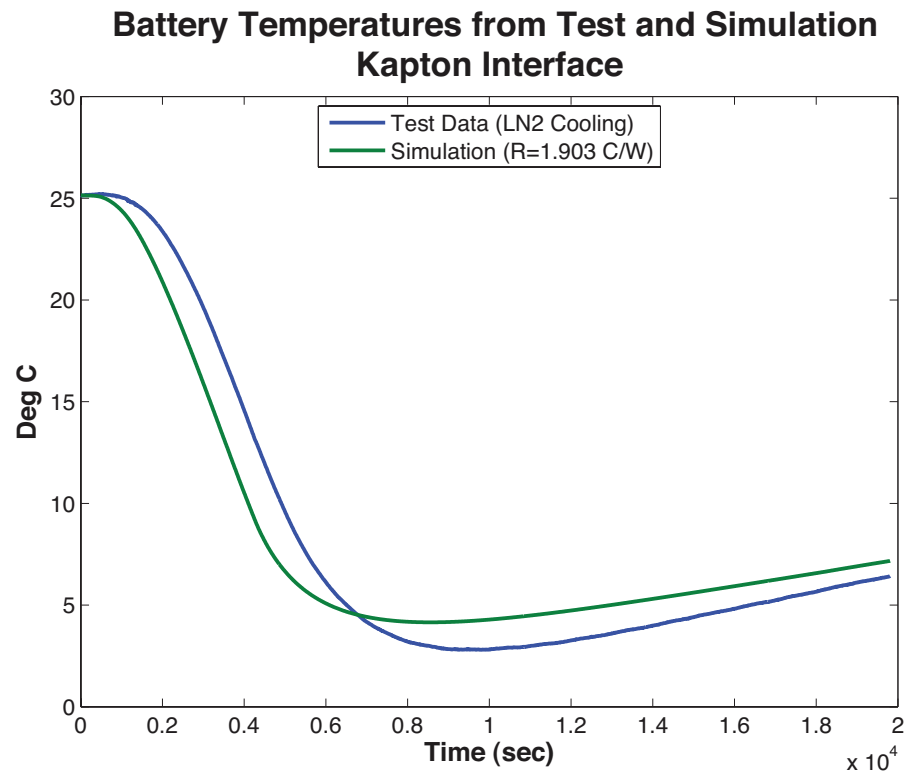


Figure 18. Simulation and Test Results for Kapton® Interface (LN2 Cooling).

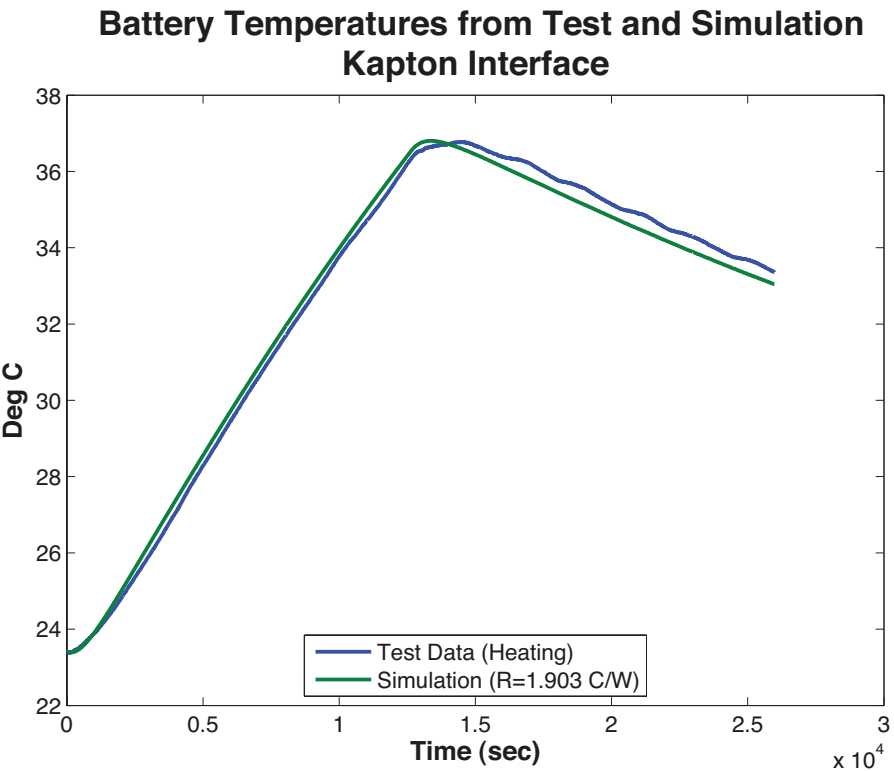


Figure 19. Simulation and Test Results for Kapton® Interface (Heating).

#### 4. Chotherm® Interface Test and Simulation

The thermal resistance for the Chotherm® material is estimated at  $R_{\text{Chotherm}} = 0.90 \text{ }^{\circ}\text{C/W}$ . Comparison plots are shown in Figure 20 and Figure 21.

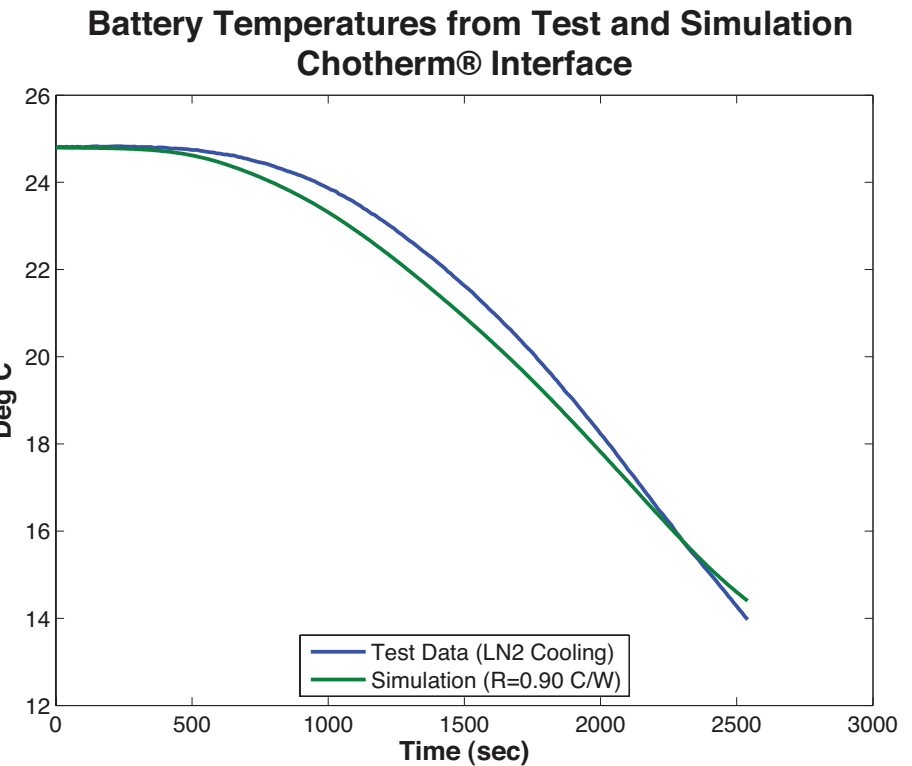


Figure 20. Simulation and Test Results for Chotherm® Interface (LN2 Cooling)

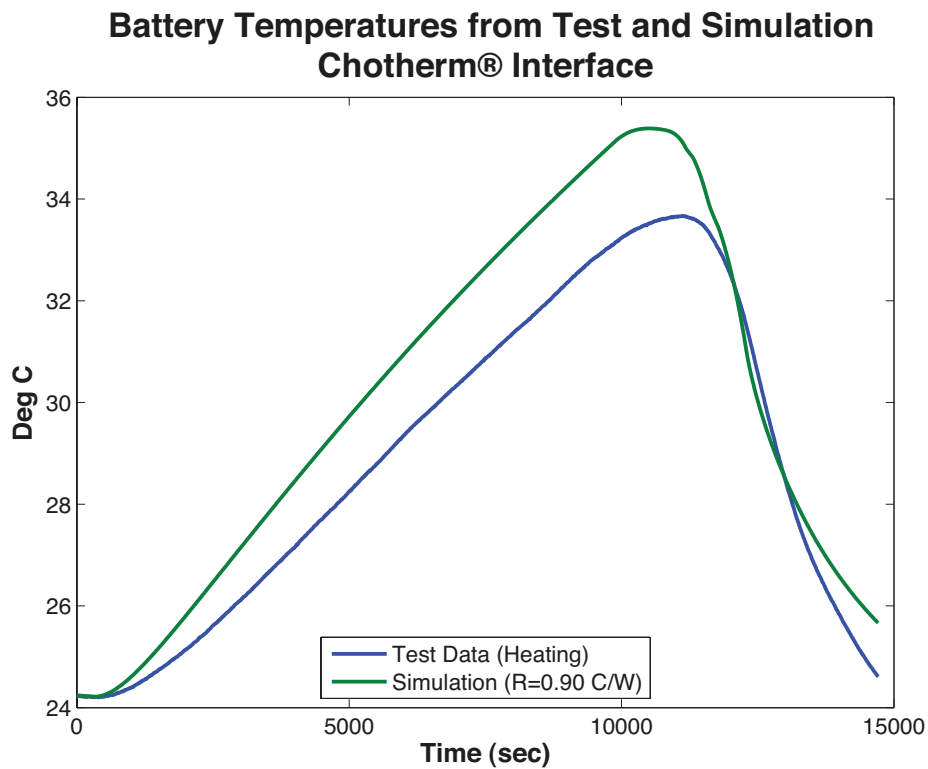


Figure 21. Simulation and Test Results for Chotherm® Interface (Heating).

## B. COMPARISON OF RESULTS AND SUMMARY

Modeling of the battery assembly and thermal interfaces using the simplified lumped capacitance model provided good agreement with the test run data. Thermal resistance values of the three interfaces are summarized in Table 2. The lumped capacitance model matched very well with the heater test run, as shown in Figure 14, where the battery temperatures for the simulation results overlay the test results. Error between the simulated thermal analysis runs and the test data were within +4°C to -8°C for the transient modeling. The metal-to-metal showed the largest error on the cold boundary condition plate.

Table 2. Summary of Thermal Interface Resistances.

Battery Thermal Capacitance	Value	Units
Lumped Mass Element	4550	J/°C
Visible Element	554	J/°C
Internal Resistance	1.0	°C/W
Thermal Interface Material		
Metal-to-Metal	0.75	°C/W
Kapton® (0.05 mm)	1.903	°C/W
Chotherm® (0.38 mm)	0.90	°C/W
Error Analysis	Max Error (°C)	Min Error (°C)
Metal-to-Metal	3.8	-7.2
Kapton® (0.05 mm)	4.0	-1.5
Chotherm® (0.38 mm)	2.0	-0.7

## IV. CONCLUSIONS

Thermal-vacuum testing of the NPSAT1 lithium-ion battery was done using known heating inputs and measuring temperature boundary conditions. Thermal modeling of the battery was then performed to match the test results, using the test data as boundary conditions, i.e., heating inputs and temperature profiles of the boundary condition plate and thermal vacuum chamber. A lumped capacitance model of the battery was created and used to model the thermal interface between the battery and its mounting surface for three different interface conditions. Agreement between the thermal model simulations and testing was achieved with differences ranging between +4°C and -8°C. The thermal contact resistances found can then be used in a larger NPSAT1 thermal model to estimate the battery temperature profiles for simulated flight operations in order to maintain the battery within operating temperature limits.

## V. REFERENCES

1. "Thermal Properties of Lithium-Ion Battery and Components," H. Maleki, S. Al Hallaj, J. R. Selman, R. B. Dinwiddie, and H. Wang, Journal of The Electrochemical Society, Vol. 146, Issue 3, pp. 947-954, 1999.
2. *Computer Aided Thermal Analysis of a Technology Demonstration Satellite (NPSATI)*, M. Gruhlke, Naval Postgraduate School Technical Report, NPS-SP-03-001, May 5, 2003.
3. "Lithium Ion Rechargeable Battery Catalog," Sony Corporation, June 2001.
4. "Thermal Behavior Analysis of Lithium-ion Batteries for Electric and Hybrid Vehicles," N. Sato, Journal of Power Sources, 99 (2001) 70-77, Elsevier Science.
5. *Spacecraft Thermal Control Handbook, Vol. I: Fundamental Technologies, 2nd Edition*, David G. Gilmore, Editor, The Aerospace Press, El Segundo, CA. 2002.
6. *Fundamentals of Heat and Mass Transfer, 4th Edition*, Frank P. Incropera and David P. DeWitt, John Wiley & Sons, New York, NY. 1981.
7. "Summary of Properties for Kapton® Polyimide Films," Dupont, 2012, [http://www2.dupont.com/Kapton/en\\_US/assets/downloads/pdf/summaryofprop.pdf](http://www2.dupont.com/Kapton/en_US/assets/downloads/pdf/summaryofprop.pdf)
8. "CHO-THERM® 1671 Thermally Conductive Elastomer Insulators" Data Sheet, Chomerics, Division of Parker Hannifin Corp., Woburn, MA, Aug. 2001, <http://www.chomerics.com/products/documents/TB45.pdf>

## **INITIAL DISTRIBUTION LIST**

1. Defense Technical Information Center  
Ft. Belvoir, Virginia
2. Dudley Knox Library  
Naval Postgraduate School  
Monterey, California
3. Research Sponsored Programs Office, Code 41  
Naval Postgraduate School  
Monterey, CA 93943
4. Space Systems Academic Group, Code SP  
Naval Postgraduate School  
Monterey, CA 93943